

<https://doi.org/10.1038/s43247-025-02603-8>

World Cultural Heritage sites are under climate stress and no emissions mitigation pathways can uniformly protect them



Zihua Chen^{1,7}, Qian Gao^{2,7}, Yajing Wu³, Jiaxin Li⁴, Xiaowei Li⁵, Xiao Li⁶, Zhenbo Wang⁴ & Haiyang Cui¹ ✉

Climate change increasingly threatens cultural heritage, yet global studies remain limited. Here we use an analytical hazard–vulnerability–exposure framework, combining global climate reanalysis and multi-model projections with site-level material inventories, to track climate stress on United Nations Educational, Scientific and Cultural Organization World Heritage sites in the past (1961–1990), present (2010–2040) and future (2070–2100). We find that 80% of sites already experience harmful heat and moisture disturbance, and nearly 19% are threatened on more than one key material such as stone and wood. A low-emission future (SSP1-2.6) could spare about 40% of at-risk sites, whereas a medium-emission (SSP2-4.5) future offers far less relief. Regional and material disparities persist, highlighting that no single mitigation pathway can uniformly protect all sites. The results guide resource prioritization and locally tailored protection strategies.

Climate change poses immediate threats to UNESCO World Heritage sites, necessitating targeted preservation strategies¹. Many sites face increasing climate-induced stress (CIS), including weather extremes and variability that often exceed the tolerance of heritage materials^{2–4}, demanding immediate adaptation strategies^{5,6}. Because heritage materials such as wood and stone respond differently to temperature and moisture swings, risk assessments must first quantify material-specific vulnerabilities before aggregating site-level CIS. Tackling these challenges aligns directly with Sustainable Development Goals (SDGs) 11 on sustainable cities and communities and 13 on climate action, emphasizing the global importance of cultural heritage preservation.

Although UNESCO and other international organizations have acknowledged climatic change as one of greatest threats to preservation of heritage values by 2016^{2–4,6,7}, ignoring material differences can misallocate conservation resources, leaving sensitive sites under protected. Meanwhile, most existing studies remain region-specific, predominantly focusing on Europe⁷, with only about 10% addressing Asia, 2% focusing on South America, and merely 1% on Africa^{8,9}. This regional bias limits the

applicability of research methods and may not translate globally¹⁰. These disparities complicate global heritage management: high-density heritage regions require precise policies to identify and prioritize the most threatened sites, while low-density regions risk being overlooked, resulting in resource allocation gaps and potential heritage losses^{9,11}. The lack of global assessments and limited scientific evidence impedes the development of effective strategies to protect sites under the escalating threat of climate change as highlighted in article 27 of UNESCO's Climate Action Policy 2023⁵.

Previous literature on the climate stress affecting cultural heritage has focused on three main aspects^{3,12}. First, sudden extreme climate events such as storm surges¹³, floods^{14–16}, landslides^{10,17} and fire¹⁸ have been studied for their immediate and prolonged effects on heritage sites. Second, gradual climate-induced degradation of heritage materials has been analyzed through dose-response models and experimental case studies, revealing how specific materials—such as limestone—deteriorate under long-term changes in temperature, humidity, precipitation and biological exposure^{19–21}. Third, research has concentrated on indoor heritage protection, emphasizing how outdoor environmental disturbances affect indoor

¹Center for Chinese Nation Research, Guizhou Minzu University, Guiyang, China. ²School of Economics, Guizhou University, Guiyang, China. ³National Engineering Research Center for Geographic Information System, China University of Geosciences (Wuhan), Wuhan, China. ⁴Institute of Geographic Sciences and Natural Resources Research, Chinese Academy of Sciences, Beijing, China. ⁵School of Urban Economics and Public Affairs, Capital University of Economics and Business, Beijing, China. ⁶Faculty of Geomatics, Lanzhou Jiaotong University, Lanzhou, China. ⁷These authors contributed equally: Zihua Chen, Qian Gao.

✉ e-mail: cuihy2004@gzmu.edu.cn

microclimates^{19,22,23}. Although many thresholds of change between heritage sites and ecosystems are not yet fully understood²⁴, these studies present an ever-present challenge to heritage sites: climate-driven changes may lead to inevitable impacts on ecosystems and eventually threaten outstanding universal values (OUV) across regions^{11,25}.

Despite these efforts, several gaps remain: (i) Many large-scale studies estimate climatic impacts based on buffer zones or coordinate points rather than actual exposed structures^{14,15}. However, site area or location does not equate to exposure from climate hazards, and misjudging the surface-air interface can lead to poor risk estimates, inefficient resource allocation, and misguided preservation decisions—especially in low income regions²⁶; (ii) Many case studies focus on single-material structures, while regional assessments often assume uniform materials—making it hard to capture how mixed-material ensembles respond differently to the same hazard. (iii) Current models do not capture country-level spatial disparities or identify where climate stress remains high or changes little under low-emission pathways such as SSP1–2.6, thereby limiting our understanding of regional vulnerability^{3,27,28}. These issues highlight challenges in implementing SDG-aligned strategies for heritage preservation, resource allocation, and adaptive governance²⁹. To address these gaps, we propose a CIS metric based on climate thresholds, providing clear risk indicators to guide equitable resource allocation^{12,30–32}.

Central to addressing these gaps is the notion of damage thresholds—quantitative climate limits for each material. Therefore, we apply a hazard–vulnerability–exposure (HVE) framework to assess changes in CIS across UNESCO cultural heritage sites. We begin by identifying material-specific thresholds (vulnerabilities) for the two main materials in historic buildings—wood and stone—as they respond differently to climate stress. For instance, existing literature reports that wood tends to crack during ~15 °C rapid cycles, while stone erodes can occur during ~10 °C cycles^{19,33,34}. Using these thresholds, we then count the frequency of CEs (hazards) exceed the limits at each site and quantify the exposed surfaces of heritage structures (exposure) using 3D building footprints³⁵, yielding a site-level CIS index. This enables us to assess threats on sites among three-time frames—the past (1961–1991), present (2010–2040), and future (2070–2100).

We map CIS for UNESCO cultural heritage sites, rank the timing and magnitude of threshold exceedance (Fig. 1), and display regional patterns (Figs. 2–3). To test what can still be protected, we run two CMIP6 pathways that bracket the policy-relevant range used by IPCC WG II: SSP1–2.6 (~1.8 °C median warming by 2100, a Paris-aligned low-emission future) and SSP2–4.5 (~2.7 °C, consistent with current pledges)³⁶. These scenarios reflect realistic planning pathways, while higher-emission scenarios offer limited immediate guidance and are thus excluded. Although over 40% sites lie in Europe and North America⁸, we pay special attention to how the same material thresholds play out across the Global North–South divide, highlighting where low- and middle-income countries face disproportionate compound-event pressure yet receive the least conservation support (Figs. 4–5). The resulting open-source dataset and scalable workflow provide a foundation for UNESCO and national agencies to prioritize adaptation investments, streamline periodic reporting, and offer future studies a reproducible global baseline.

Results

Global-scale risk and potential rescue of UNESCO heritage

Hereinafter, ‘threat’ refers to the observed change in CIS from 1961–1991 to 2010–2040, driven purely by observed climate trends and excluding any on-site adaptation. ‘Mitigation benefit’ is the 2070–2100 reduction in CIS (Avoided-CIS) if the world follows SSP1–2.6 rather than SSP2–4.5, thereby isolating emission-pathway effects and likewise ignoring local measures. SSP1–2.6 (~1.8 °C) and SSP2–4.5 (~2.7 °C) bound the warming range highlighted by IPCC WG II (see “Methods: Future scenario simulation”).

Key findings at a glance. Figure 1 highlights global hotspots of threatened CIS on UNESCO cultural heritage driven by climatic CEs, along with the potential to mitigate these impacts under a low-emission

pathway. Our analysis shows that 19% UNESCO sites currently experience CIS levels that exceed thresholds for both stone and wood—a condition intensified by CEs—when comparing 1961–1991 to 2010–2040. If the world follows SSP1–2.6, ~9.7% of these sites at dual-material vulnerability risk could experience substantial relief from CIS in 2070–2100. These insights underscore the critical role of heritage conservation, climate adaptation, and disaster risk management in safeguarding culturally important sites, aligning with global sustainability efforts under the Paris Agreement and the SDGs.

Major regional hotspots. Four regions emerge as notable hotspots where acute stress or mitigation benefit is especially pronounced:

- **Central and Eastern Europe:** Despite having relatively flat exposure slopes (as indicated by k in Fig. 1a, showing that TEA does not drastically change SEA), accelerating heatwaves and heavy precipitation lead up to 44 sites exceeding stress thresholds. Encouragingly, many of these sites could benefit greatly under SSP1–2.6, suggesting that proactive climate policies can be pivotal in reducing CIS.
- **Arab States & South America:** wood- is not yet severely threatened, but even the low-emission scenario brings only modest preservation. This underscores gaps in adaptive capacity—beyond emission reductions alone—and calls for heightened disaster risk management plans tailored to local cultural and climatic realities.
- **Africa:** African sites exhibit high intercepts in total and specific exposure (b in Fig. 1a), meaning even smaller sites have sizeable vulnerable footprints. Fewer than 30% of these sites show mitigation benefit under SSP1–2.6, emphasizing the pressing need for robust, region-specific adaptation strategies in historically under-resourced areas.
- **North America:** Although overshadowed in terms of total UNESCO site count compared to Europe or Asia, North America shows the greatest preservation potential under a low-emission trajectory: around 72% of stone structures and 44% of wood structures could see meaningful CIS reductions. This contrast with the region’s previously mixed climate policy record spotlights the global gains achievable through more rigorous intervention.

Time-evolving threats and mitigation benefits under different pathways

After discussing global hotspots, we now quantify how cultural heritage have already been affected by climate change and how much impact could still be avoided by presenting the full maps of heritage sites with Δ CIS.

Cultural heritage already affected (past vs. current). By using the past period (1961–1991) as a baseline³⁷, we quantified shifts in CIS for the current era (2010–2040). Figure 2 shows the Δ CIS_{current–past}—where a positive value indicates rising CIS and a negative value suggests easing conditions. Overall, 80% of sites exhibit increased CIS in either wood or stone thresholds, and 19% face dual-material vulnerability—meaning both stone and wood thresholds are exceeded, likely driven by heatwaves and extreme precipitation. This proportion highlights the broadening impact of climate variability, affecting not only recognized hotspot areas in result 1, but also emerging regions under stress.

- **Inland Regions Intensifying:** Although Result 1 has already identified Europe and parts of Asia as key clusters, the Δ CIS_{current–past} specifically shows that inland regions (such as central Europe) often experience moderate to severe stress, consistent with intensifying CEs away from coastal microclimates. In Asia, 11.45% of sites already exceed both material thresholds, especially across Central China and Central Asia. This observation is aligned with previous studies^{31,38}, which have highlighted similar patterns of heightened climate-induced stress in inland regions.
- **Emerging Stressors:** In semi-arid or tropical zones—such as parts of southern Africa and South America—site density may be lower, but many locations report substantial CIS increases. This escalation aligns

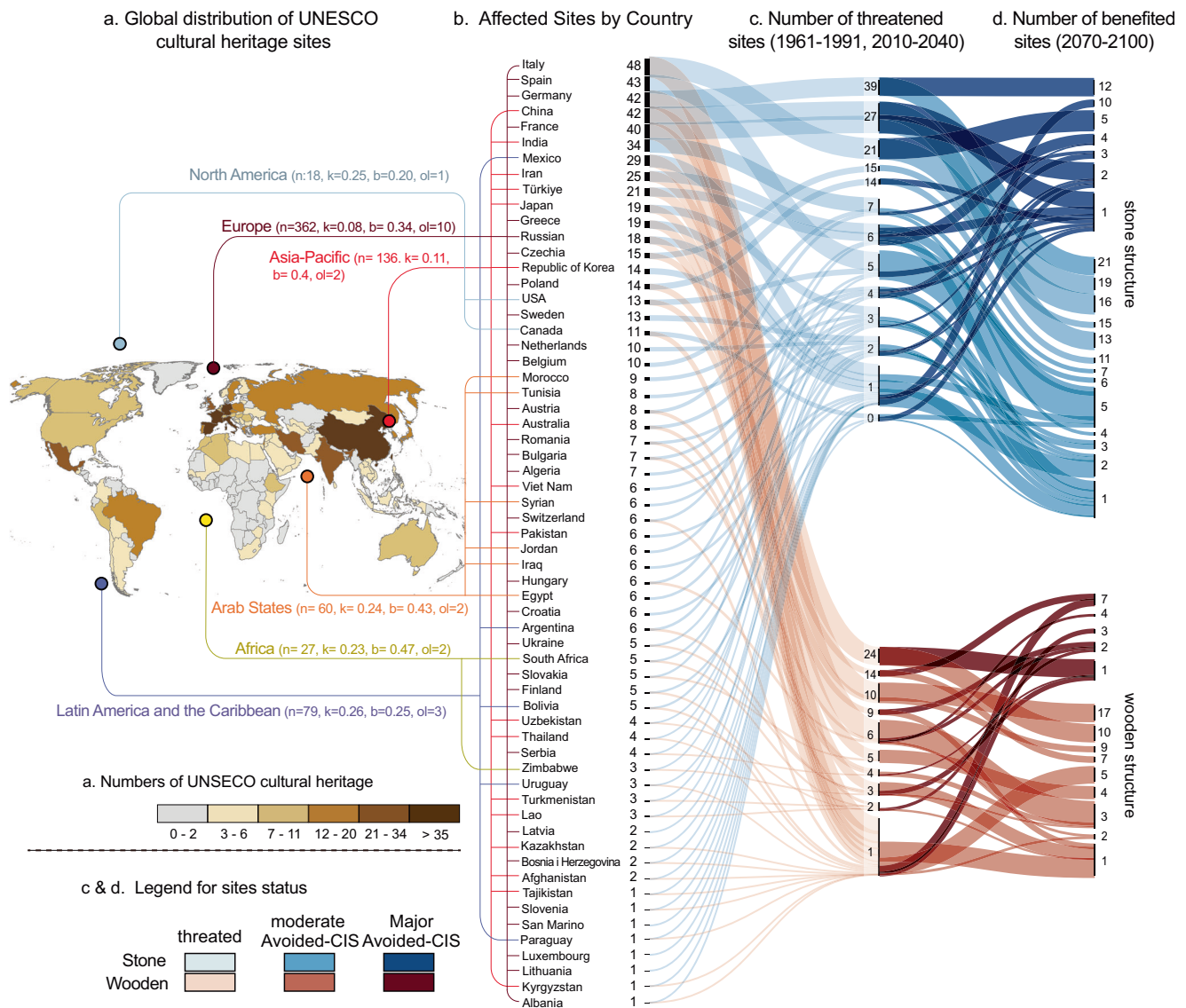


Fig. 1 | Global hotspots and mitigation benefits for UNESCO cultural heritage. **a** Map of UNESCO cultural-heritage sites (n). For each continent, we plot TEA on the x -axis against SEA (TEA/ground area) on the y -axis and report the fitted slope (k), which shows how unit-area exposure changes as total exposed surface grows. A low k (≈ 0.08 in Europe) indicates that very large sites gain little additional SEA—typical of horizontally extensive yet low-rise ensembles. A high k (≈ 0.25 – 0.26 in the Americas) means larger TEA is accompanied by proportionally higher SEA, implying taller or more densely packed structures. The intercept (b) gives the expected SEA of a minimally sized site. Outliers (ol) that fall outside the TEA–SEA trend are kept for transparency. Detailed continent-level regressions are shown in

Supplementary Fig. 1. **b** Listed countries are those facing threats in CIS on any material under the current scenario (current vs. past) and showing mitigation benefit under the future scenario (SSP2-4.5 vs. SSP1-2.6). **c** Number of sites with any material (current vs. past) has exceeded thresholds due to CEs, comparing the period 2010–2040 to 1961–1991. **d** Number of sites with positive Avoided-CIS under SSP1–2.6, indicating how reduced emissions can lower the exceedance of material-specific thresholds for both stone and wood heritage structures (See “Methods, Step 7 for Δ CIS categorization rationale”). Map generated with ArcGIS Pro 3.2 (Esri). Country boundaries: RESDC, CAS, <https://www.resdc.cn/data.aspx?DATAID=205>.

with frequent heatwaves, drought, and extreme heat events that intensify material weathering and structural decay³⁹.

- **Implications:** This historical-to-current shift clarifies which areas have already experienced accelerated degradation, underscoring how regional climatic trends can magnify or moderate existing vulnerabilities. By pinpointing these early-warning signals, conservation efforts can be better prioritized, especially for sites not covered in the hotspots of Result 1.

Heritage mitigation benefit (avoided-CIS, SSP2-4.5 vs. SSP1-2.6). Looking ahead to 2070–2100, Fig. 3 assesses potential gains if the world adopts a low-emission pathway (SSP1-2.6), contrasting it with a moderate emission trajectory (SSP2-4.5). Rather than re-examining the same regional patterns in detail, we focus on overall mitigation benefit in CIS

and the geographic pockets most likely to benefit from robust emission cuts. Our analysis indicates that up to 40% of UNESCO sites can achieve marked CIS relief under SSP1-2.6, reinforcing the practical payoff of ambitious climate mitigation. Even for regions not currently facing the most extreme conditions, efforts to limit warming can still mitigate future CEs, thereby benefiting the conservation of cultural heritage.

- **Benefits for Sites with Less Severe Stress:** For instance, many North American sites, though moderate in current CIS levels⁴⁰, could see 36% achieve positive shifts under SSP1-2.6. This echoes findings from Result 1, showing that even areas with fewer heritage assets or historically milder extremes still gain from stringent mitigation pathways.
- **Stronger Impact near Major River Basins:** Certain river-basin or lowland areas—such as the Yangtze Basin in China, the Lower Danube Plain in Europe, and the Río de la Plata Basin in South

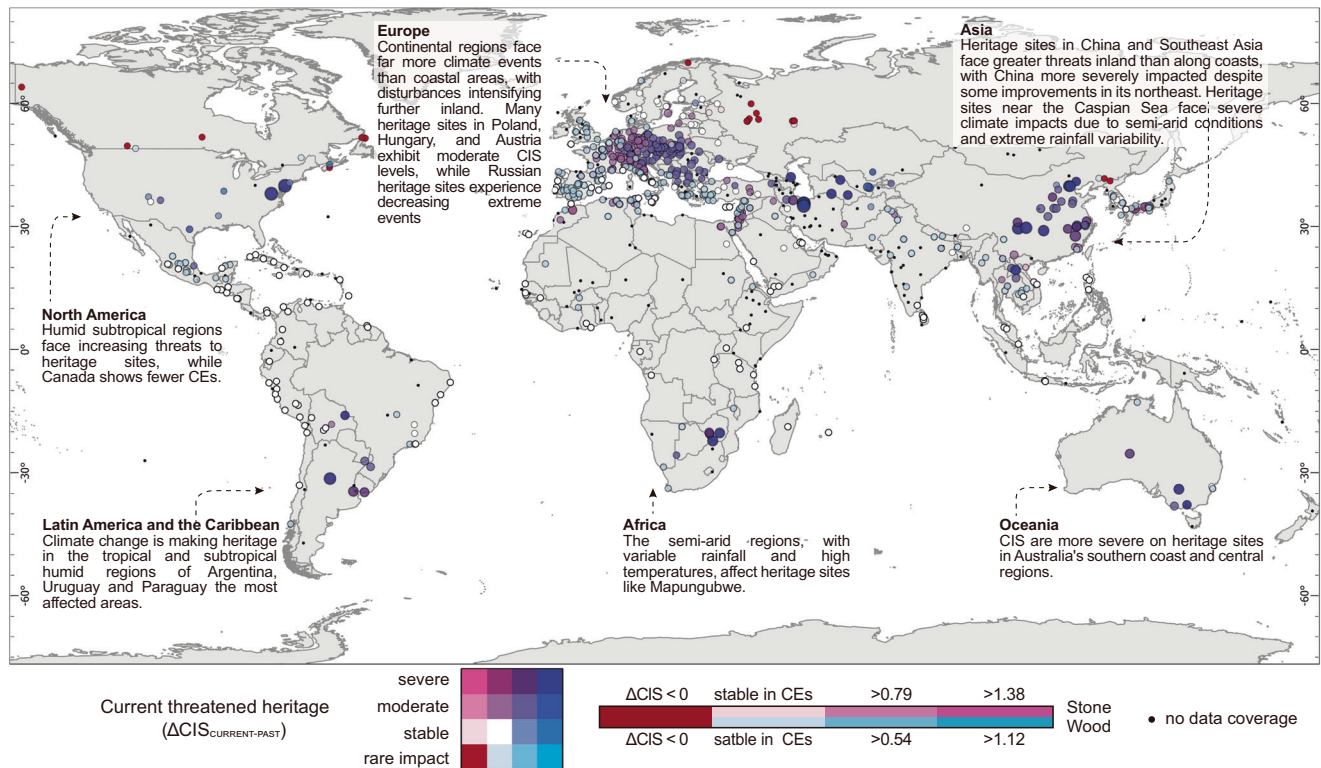


Fig. 2 | Spatial distribution of threatened cultural heritage sites ($\Delta\text{CIS}_{\text{current-past}}$). $\Delta\text{CIS}_{\text{current-past}}$ captures only the rise in CEs since 1961, excluding non-climatic stressors such as, e.g., tourism, regional pollution. Consequently, the true risk may be

higher at heavily visited or poorly managed sites (See “Methods, Step 7 for ΔCIS categorization rationale”). Map generated with ArcGIS Pro 3.2 (Esri). Country boundaries: RESDC, CAS, <https://www.resdc.cn/data.aspx?DATAID=205>.

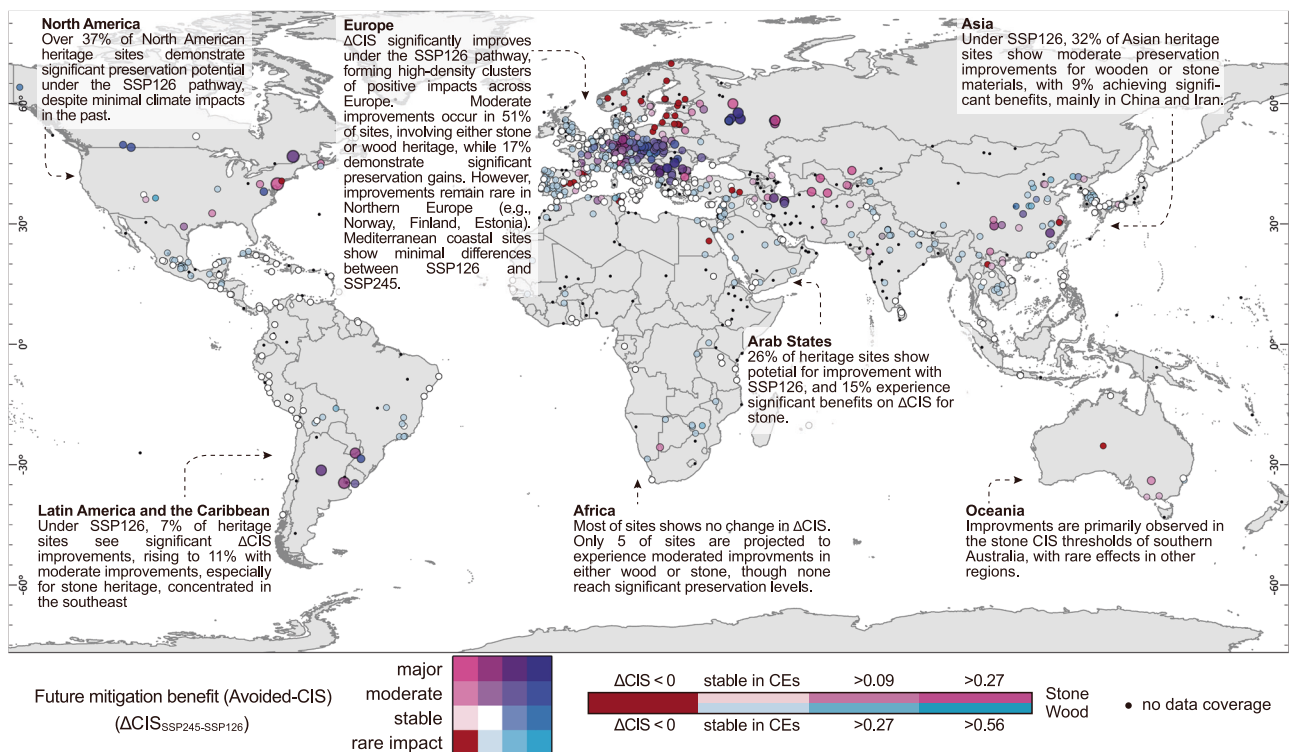


Fig. 3 | Spatial distribution of mitigation benefit (Avoided-CIS): SSP2-4.5 vs. SSP1-2.6. $\Delta\text{CIS}_{\text{SSP245-SSP126}}$ gives each site's mitigation benefit (Avoided-CIS). Larger positive values indicate greater avoided stress, whereas near-zero or negative values mark areas where mid- and low-emission pathways yield similar outcomes.

Avoided-CIS consider only reduction of CEs (temperature-then-humidity) and exclude non-climatic stressors (See “Methods, Step 7 for ΔCIS categorization rationale”). Map generated with ArcGIS Pro 3.2 (Esri). Country boundaries: RESDC, CAS, <https://www.resdc.cn/data.aspx?DATAID=205>.

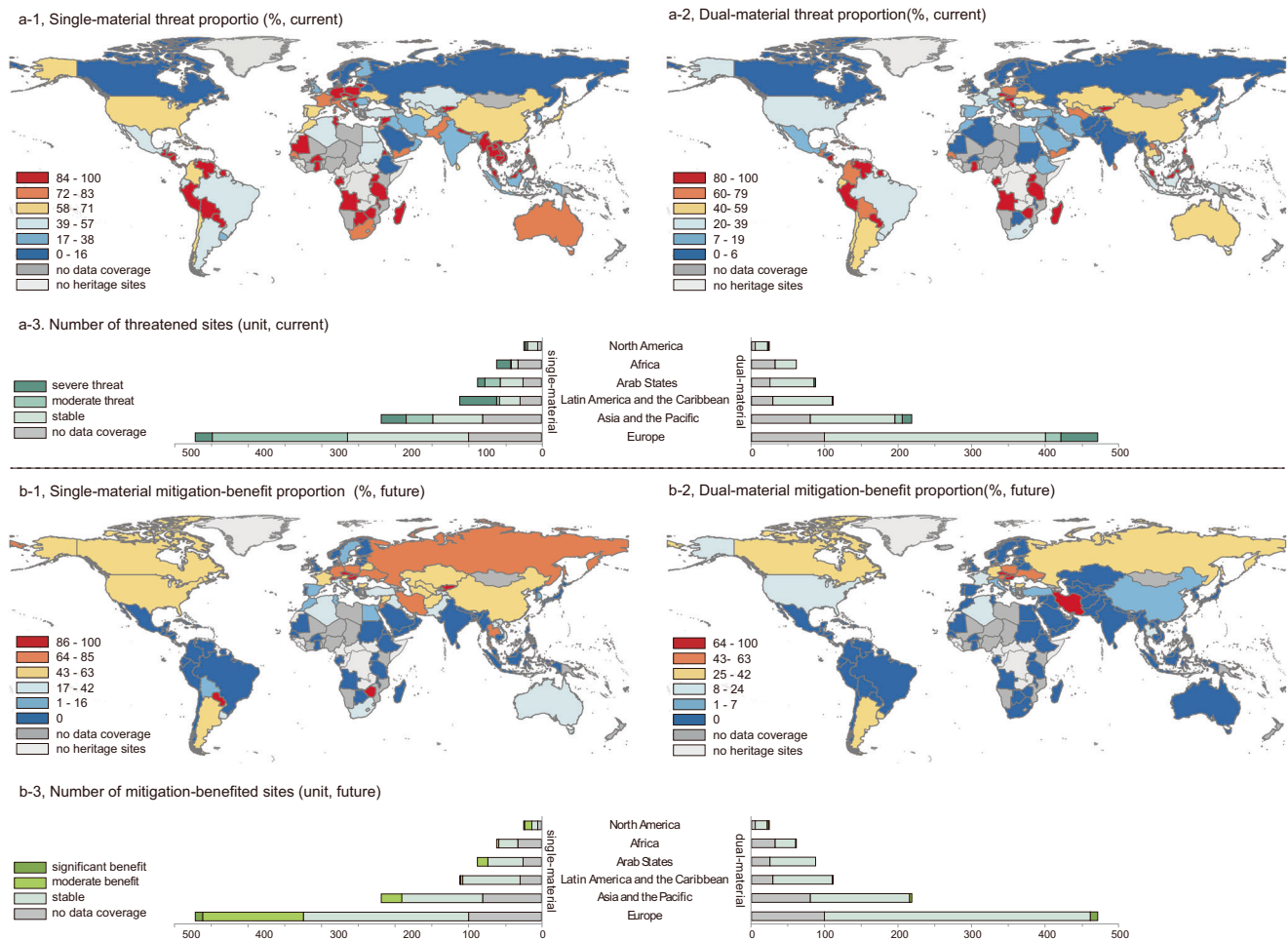


Fig. 4 | Country-level proportions of threatened vs. benefited sites. This figure summarizes the status of UNESCO cultural heritage sites under the current climate window (2010–2040) and the future low-emission pathway SSP1-2.6 (2070–2100). Percentage of sites where either stone or wood exceeds its threat threshold (**a-1**) or attains a mitigation benefit (**b-1**). Percentage of sites where both stone and wood simultaneously exceed threat thresholds (**a-2**) or both

record mitigation benefits (**b-2**). Absolute numbers of threatened (**a-3**) and mitigation-benefited (**b-3**) sites aggregated by continent. For data processing and threshold definitions, see “Methods”. Map generated with ArcGIS Pro 3.2 (Esri). Country boundaries: RESDC, CAS, <https://www.resdc.cn/data.aspx?DATAID=205>.

America—stand out for strong potential for preservation. In these locales, adopting SSP1–2.6 notably reduces the frequency of threshold-exceeding climate events, delivering more stable conditions for both materials.

- **Minimal Gains in Some Regions:** However, parts of the Southern Hemisphere and Northern Europe register modest changes, implying that current climate (semi-arid or high-latitude) does not diverge drastically between SSP2–4.5 and SSP1–2.6. Researchers have suggested that in Northern Europe, for instance, snow cover dynamics and nighttime warming patterns reduce the relative difference in extreme events between low- and medium-emission scenarios^{41–43}.

Why do some sites fare worse or better?

To clarify the factors influencing CIS in UNESCO heritage sites, we applied a panel regression model (Table 1) that evaluates exposed area, CEs, and their interactions (see “Methods 4”). Below, we synthesize four key insights drawn from our analysis under both SSP1–2.6 and SSP2–4.5.

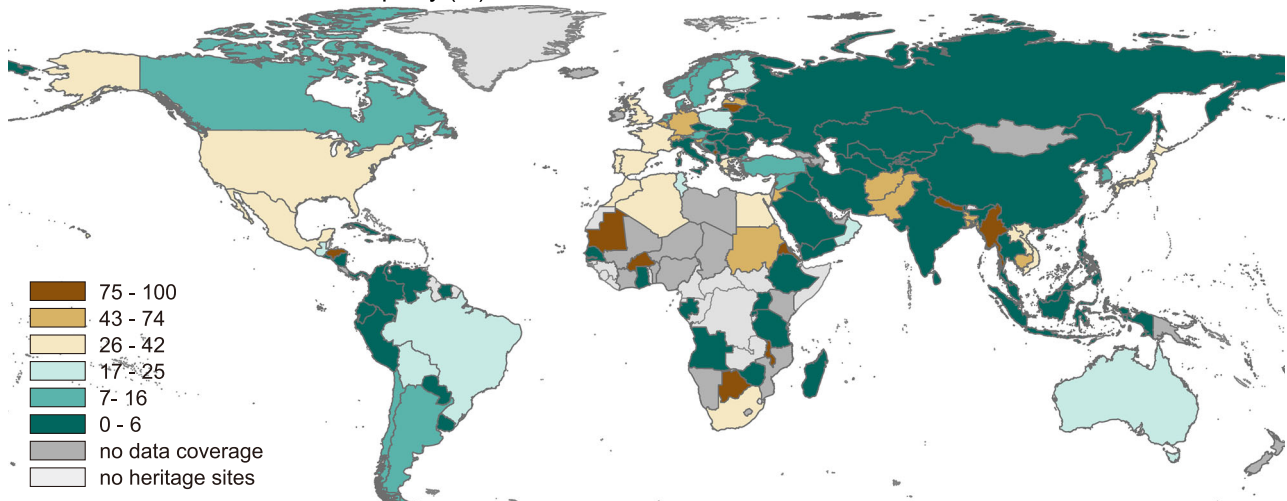
Heritage faces steadily intensifying climate pressure. Our regression analysis shows that CIS has markedly increased over time (see Table 1, $\gamma_{current}$ vs. γ_{future}), especially under SSP2–4.5. Assuming all other factors remain constant, wood-based sites may see an estimated 40% CIS rise

under SSP1–2.6 and 62% under SSP2–4.5 from the past (1961–1991) to the current/future period, while stone-based sites could experience even larger increases (114% and 116%). These estimates imply that both stone and wood heritage are at heightened risk of damage from more frequent or intense compound events (CEs), underscoring the need for early climate adaptation measures.

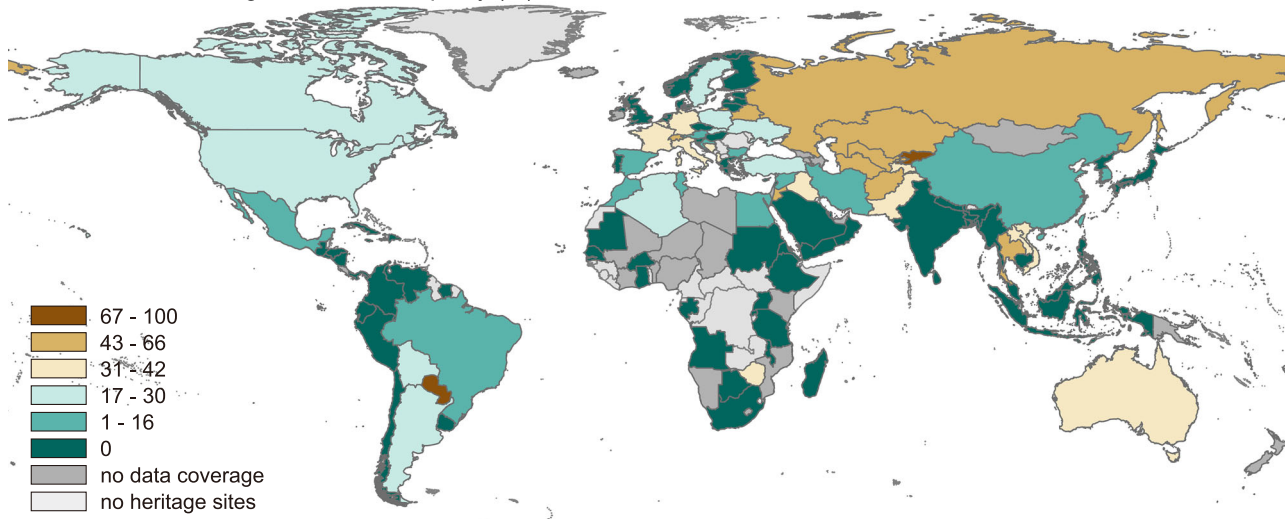
Specific exposed area matters more than total size. Positive β_{SEA} values across all models confirm that sites with larger specific exposed surfaces, regardless of total site size, are more prone to climate-induced damage. Therefore, conservation efforts should prioritize zones with high SEA (e.g., improved drainage or protective barriers), as these high-exposure areas have the greatest vulnerability to repeated stress events.

Wood-based heritage faces greater repeated-stress vulnerability. The positive $\theta_{current}$ for wood (e.g., 0.0086**) indicates that wooden heritage deteriorates more severely with repeated climate disturbances, whereas stone sites (with negative $\theta_{current}$) show a reduced rate of increasing vulnerability over time. This outcome suggests that wood structures may require sustained maintenance interventions (e.g., sealing, anti-rot treatments), while stone sites may benefit from periodic structural reinforcement.

a. Stone–wood current threat disparity (%) — current



b. Stone–wood mitigation-benefit disparity (%) — future



c. Stone–wood disparity in site counts (unit)

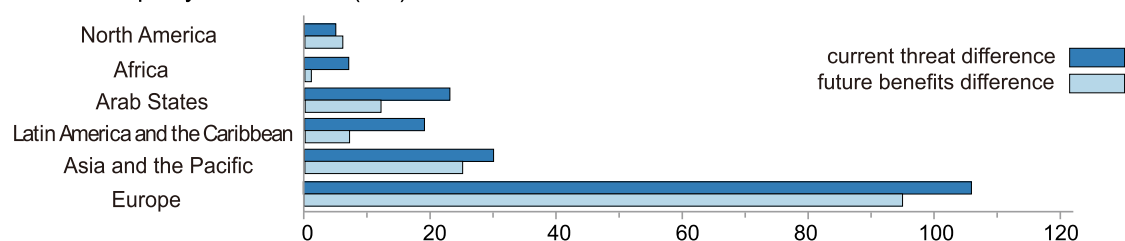


Fig. 5 | Country-level material-specific threats and mitigation benefits. **a** The value is the absolute difference between the numbers of stone and wood sites currently under climatic threat, divided by the total number of UNESCO cultural sites in each country (2010–2040). Higher percentages denote larger material-specific vulnerability gaps. **b** The value is the absolute difference between the counts of stone and wood sites with positive mitigation benefits (Avoided-CIS) under SSP1–2.6, expressed as a percentage of each country’s total UNESCO cultural sites for

2070–2100. Higher percentages highlight uneven benefits from emission mitigation. **c** Absolute disparity in site counts between stone and wood: blue bars show current threats (2010–2040), and light-blue bars show future mitigation benefits (Avoided-CIS, 2070–2100). For data processing steps and threshold definitions, see “Methods”. Map generated with ArcGIS Pro 3.2 (Esri). Country boundaries: RESDC, CAS, <https://www.resdc.cn/data.aspx?DATAID=205>.

Larger wooden sites demonstrate higher adaptive resilience. The negative β_{SEA*CE} for wood indicates that larger wood-based sites, despite having extensive exposed surfaces, often incorporate architectural or conservation features that help offset climate extremes. As a result, adaptive policies (e.g., roof overhangs, elevated foundations) can lower the effective exposure per unit area, offering a viable strategy to enhance

resilience for big, complex heritage sites in moderate- to high-emission contexts.

National disparities in threats and mitigation benefits

Threat and mitigation benefits. A deeper country-level analysis clarifies how policy responses may vary. Our findings show that Southern

Table 1 | Regression results of CIS across time frame between materials

Sample/Coef.	β_o	β_{SEA}	β_{CE}	β_{SEA+CE}	$\gamma_{current}$	γ_{future}	$\theta_{current}$	θ_{future}
SSP1-2.6 Stone	19.3310***	0.1594**	0.0062***	0.0001	0.5807***	1.1372***	-0.0008**	-0.0030***
SSP1-2.6 Wood	17.6465***	0.1559*	0.0307***	-0.0012	0.2845***	0.3987***	0.0086***	0.0060***
SSP2-4.5 Stone	19.3116***	0.1598**	0.0062***	0.0002	0.5665***	1.1600***	-0.0007**	-0.0031***
SSP2-4.5 Wood	17.6041***	0.1486*	0.0338***	-0.0015**	0.3272***	0.6191***	0.0086***	0.0026*

* $p < 0.1$.** $p < 0.05$.*** $p < 0.01$.

Hemisphere nations often exhibit high proportions of threatened heritage sites—whether in stone or wood (Fig. 4-a) or dual-materials (Fig. 4-b). By contrast, certain Northern Hemisphere regions (such as Central Europe, Southeast Asia, and North America) have high proportions of heritage sites threatened in at least one material, but far fewer with dual-material vulnerabilities.

Under future scenarios (Fig. 4b-1), adopting SSP1-2.6 yields the most notable mitigation benefit (Avoided-CIS) across large parts of Eurasia, even where current climate stress is minimal. For example, Russia and many Central Asian states show above 64% mitigation benefits in either stone or wood heritage, while Argentina, Uruguay, and Zimbabwe also demonstrate strong preservation potential). However, the proportion of sites with dual-material preservation remains below 25% in most countries, with exceptions in Iran and a few Central European nations, including Hungary, Czech Republic, and Austria (Fig. 4b-2).

Although the low-emission pathway delivers substantial overall mitigation benefits for heritage, major challenges remain. Across all continents except North America, the number of possible preserved heritage sites under SSP1-2.6 falls short of the number currently affected (a-3 vs. b-3). Furthermore, the number of sites where both stone and wood exhibit simultaneous preservation potential are notably low—Europe leads with 36 sites, followed by Asia with only 5 sites. This indicates that under SSP1-2.6, the frequency of future compound climate events exceeding the reference thresholds for both materials is marked reduced. These discrepancies highlight that even under ambitious mitigation efforts, many regions face complex heritage challenges linked to distinct material vulnerabilities. Consequently, we next explore how variations in stone-wood vulnerabilities shape divergent management needs.

Divergent material vulnerabilities and gaps. Comparisons of stone vs. wood at the country level reveal moderate discrepancies under current conditions, yet these disparities can widen substantially. For example, Central Asia and Russia report relatively high mitigation-benefit rates under SSP1-2.6 (Fig. 4) but show 67–100% differences between stone and wood preservation. In future scenarios, regions with large proportional disparities shift from Africa, South Asia, and North America to Central Asia and Russia, where material-specific differences account for up to 43% of the total heritage sites.

Figure 5c highlights the absolute differences in preservation between materials. All continents, except North America, show marked reductions in material-specific disparities under SSP1-2.6, suggesting that most regions would benefit from mitigation efforts, although spatial disparities persist (Fig. 5b). In contrast, North America shows an increase in the absolute difference between stone and wood preservation compared to current threat scenarios. This trend aligns with the earlier finding in Result 3.2, where many heritage sites in North America exhibited Δ CIS as rare impact (see Fig. 3). These results emphasize that no single pathway uniformly benefits all heritage types. In some countries, stone heritage might be better preserved while wood lags behind—or vice versa. As highlighted earlier, reducing emissions alone cannot guarantee comprehensive protection, therefore, it is necessary to incorporate material-specific thresholds into risk assessments to ensure cultural heritage receive tailored interventions suited to local conditions.

Discussion and conclusion

World Cultural Heritage properties stand as remarkable achievements of humankind and serve as evidence of our shared intellectual history. By employing an HVE assessment framework, we show that nearly 80% of UNESCO cultural heritage sites are now subject to threats from CEs, and that a Paris-aligned pathway (SSP1-2.6) could still spare roughly 40% of those otherwise on course for severe degradation by 2070–2100. These global figures mirror the threat recently documented for natural World Heritage sites¹, while extending the warning to cultural assets and, crucially, to low income regions that earlier regional surveys left largely uncharted.

A central message of our analysis is that CIS on cultural heritage is neither uniform nor linear: it varies sharply by place, period and materials. Some regions that shoulder today's heaviest CEs loads—parts of coastal East Asia and northern Australia—level off or even ease later in the century (Fig. 2), while risk escalates in Central Asia, the tropical Andes and much of Central Europe (Supplementary Fig. 2). Materials diverge just as strongly. Limiting warming to $\sim 1.8^\circ\text{C}$ (SSP1-2.6) by 2070–2100, instead of $\sim 2.7^\circ\text{C}$ (SSP2-4.5), reduces threshold-exceeding CEs by $\sim 13\%$ for stone and $\sim 25\%$ for wood—so while mitigation may slow salt crystallization and frost-splintering in stone, many wooden structures could still exceed their decay thresholds. Deterioration accelerates in areas where CEs cluster, leaving visible signs such as black gypsum crusts on façades exposed to pollution and frequent wetting⁴⁴. This crust signals advanced sulphation, traps moisture, and ultimately requires abrasive cleaning that erodes original materials and accelerates loss. Over time, such cumulative degradation threatens the integrity and authenticity that underpin the Outstanding Universal Value (OUV) of affected heritage sites.

Our findings carry important implications for climate justice and preservation planning. First, exposure and relief are uneven: in most southern African states, along the Pacific coast of South America, and across much of Southeast Asia, more than four-fifths of sites have already experienced high-frequency CEs that contribute to CIS threats (Fig. 4a). Even if end-century warming is held near 1.8°C , countries such as Zimbabwe, Paraguay, and Kyrgyzstan still show roughly 80% of their cultural assets under severe CIS (Fig. 4b). Second, from 1961 to the present, material-specific CIS disparities—between stone and wood—are most pronounced in regions with limited conservation capacity (Fig. 5). This raises concern because these regions, in many cases, lack the technical capacity and policy support needed to address the challenges—unlike Germany, Italy or China, which, though facing larger absolute numbers of high-CIS sites (Fig. 2), benefit from greater technical and financial resources. Point-cloud scanners, micro-climate loggers, and teams of trained conservators—standard kit in Paris or Beijing—remain rare in many low-resource and island-state settings, where digital mapping infrastructure might be still limited.

Accordingly, a tiered support framework for cultural heritage, grounded in multilateral climate finance mechanisms, is needed. Key instruments include: (i) allocating a dedicated window within the UNFCCC Loss-and-Damage Fund for heritage risk reduction in low-income countries, prioritizing smaller or lesser-known sites with high SEA values; (ii) listing cultural assets as eligible under the Green Climate Fund so adaptation finance can reach vulnerable sites; and (iii) creating flying-lab consortia under ICOMOS and ICCROM to circulate 3-D documentation kits, remote-sensing expertise, and on-site training across regions, in partnership

with local stewards. These proposals are not merely technical fixes; they reflect a deeper political reality. While responsibility for heritage protection has traditionally fallen to national governments, however, this model breaks down under climate pressure. Many low-income countries face impossible trade-offs between safeguarding cultural assets and meeting urgent demands in housing, health, and climate resilience. Just as climate change is the world's largest market failure, so too is the under-financing of cultural adaptation: emissions are concentrated in wealthier countries, but the cultural losses fall disproportionately on lower-income regions that lack the means to assess, document, or protect what is at risk. Therefore, redirecting multilateral climate finance toward heritage is not a luxury—it is a structural correction long overdue. Such targeted, cooperative investment would prevent cultural heritage in low income countries from becoming an unseen casualty of the climate crisis, and would align preservation with SDG principles on climate justice, equity, and shared stewardship^{4,45}.

We acknowledge several limitations. First, our projections isolate the emissions dimension of climate policy and do not include on-site adaptation such as drainage or protective shelters; real-world risk may therefore be lower where such measures exist—or higher where they are absent. Second, we use building footprints as proxies for heritage value, yet intangible traditions and sacred landscapes can erode long before structural damage is visible, underscoring the need for community-based ethnographic monitoring. Third, the climate stressors are limited to daily temperature and humidity, excluding hazards like storm surges and wildfire^{10,15–18}. A future meta-analysis that merges multiple hazard types could establish shared benchmarks and sharpen the prioritization of site-specific interventions.

Methods

We followed a seven-step workflow based on the HVE framework to quantitatively assess CIS on UNESCO cultural heritage sites (Fig. 6)^{10,46}. In this framework, *hazard* refers to CEs that could damage heritage materials, *vulnerability* denotes the susceptibility of those materials (e.g., wood or stone) to climatic extremes as determined by their physical properties and damage thresholds, and *exposure* represents the extent to which heritage assets are subject to these hazards (e.g., the surface area of structures exposed to air). Using this HVE approach, we integrated diverse datasets and sequentially evaluated each component—climatic hazards, material vulnerabilities, and site exposure—and then combined them into a composite CIS index. Finally, we compared CIS outcomes across different time periods and emission scenarios to identify temporal trends and spatial disparities. The detailed procedure is outlined below.

Step 1. Data compilation

Climate data. 2 m surface air temperature and relative humidity fields at 0.1° resolution across three 30-year periods—past (1961–1991), present (2000–2030), and future (2070–2100) from the European Centre for Medium-Range Weather Forecasts (ECMWF) via the Copernicus Climate Data Store^{47,48}—are used to quantify (i) the additional CIS that has already emerged and (ii) the proportion that could be avoided under ambitious mitigation scenarios.

Heritage site data. UNESCO's cultural heritage data are sourced from the official UNESCO World Heritage List as of June 2024 (<https://whc.unesco.org/en/list>). Out of 1,200 World Heritage sites, we focus on 938 sites classified as cultural or mixed (both cultural and natural) heritage. Sites without built structures—such as caves, murals, archeological sites, and prehistoric traces—are excluded since our study aims to investigate the impact of climate on human architectural footprints. These sites are labeled as no data coverage in the Figs. 2 and 3. The overall global average effective coverage is 74%, primarily due to limited satellite imagery availability.

3D building footprints. Building footprint and height data were obtained from the latest global 3D-GloBFP building database. Footprints come from Microsoft and Google datasets, whose heights are predicted with XGBoost model trained on four reference sets (ONEGEO, Microsoft,

Baidu, and EMU)^{35,49}. Independent validation reports median RMSE ≈ 2.7 m and $R^2 = 0.89$, i.e., >90% of heights fall within ±3 m (validation sample ≈ 1.7 billion built structures), showcasing higher accuracy compared to other global height products³⁵.

Step 2. Climatic hazard assessment

Using the climate data, we identified and quantified CEs at each site as the primary climatic hazards^{7,50,51}. CEs are defined solely by temperature- and humidity- disturbance threshold exceedances^{39,52}, within a 3-day window. Both the European Climate for Culture protocol and laboratory tests indicate that temperature-humidity swings occurring within 3 days trigger the most severe damage in heritage materials^{30,53,54}. This yields an annual CE count per site, which we average over each 30-year slice to provide the hazard term in Eq. 4.

$$CE_{ij} = \sum_{d=1}^{365} 1(|\Delta T_{d,d-N}| > T_{\theta} \wedge |\Delta RH_{d,d-N}| > RH_{\theta}) \quad (1)$$

where i indexes the heritage site, y the calendar year, $n \in \{1, 2, 3\}$ days, and T_{θ} , RH_{θ} are material-specific impact thresholds identified in step 3.

Step 3. Material vulnerability analysis

Next, we evaluated the vulnerability of each site's construction materials to the identified hazards. We focused on the two most prevalent heritage materials—wood and stone^{27,55}—and applied established thermal and moisture tolerance thresholds for each^{56,57}. Specifically, we used literature-based criteria for what constitutes a damaging temperature swing or humidity change for wood and stone (Table 2). For every extreme event identified in Step 2, we determined whether the intensity and rate of change would surpass the material-specific degradation thresholds. This analysis results in a vulnerability profile for each site, indicating how susceptible its materials are to the recorded climate extremes (a higher frequency of threshold exceedance signifies greater vulnerability).

Step 4. Heritage exposure analysis

Using the 3-D GloBFP building dataset clipped to each UNESCO buffer (<https://whc.unesco.org/>), we quantified how much fabric at every site is directly exposed to weather⁵⁸. For every heritage site, based on area-weighted mean height (Eq. 2), we calculated the Total Exposed Area (TEA)—the total exposed surface area of all structures (Eq. 3). Because TEA naturally grows with the horizontal extent of a site, we also report the Specific Exposed Area (SEA)—TEA divided by ground area to capture differences in construction density and height, not merely footprint size (Eq. 4).

$$\text{Weighted Height}_i = \frac{\sum (H_j \times A_j)}{\sum A_j} \quad (2)$$

$$\text{Total Exposure Area(TEA)}_i = \text{Weighted Height}_i P_i + A_i \quad (3)$$

$$\text{Specific Exposure Area(SEA)}_i = \frac{\text{TEA}_i}{A_i} \quad (4)$$

where H_j and A_j are the height and footprint of building j within site i . P_i is the perimeter length of site i . A larger or more spread-out site might have a high TEA but a lower SEA, indicating that increasing size does not proportionally increase unit-area exposure. For detailed insights into the relationship between TEA and SEA across continents, refer to Supplementary Fig. 1.

Step 5. CIS calculation

We calculate the CIS using the exposed area of the heritage i and the frequency of Climatic CEs, ensuring consistency with previous analyses that emphasize the significance of both heritage exposure and

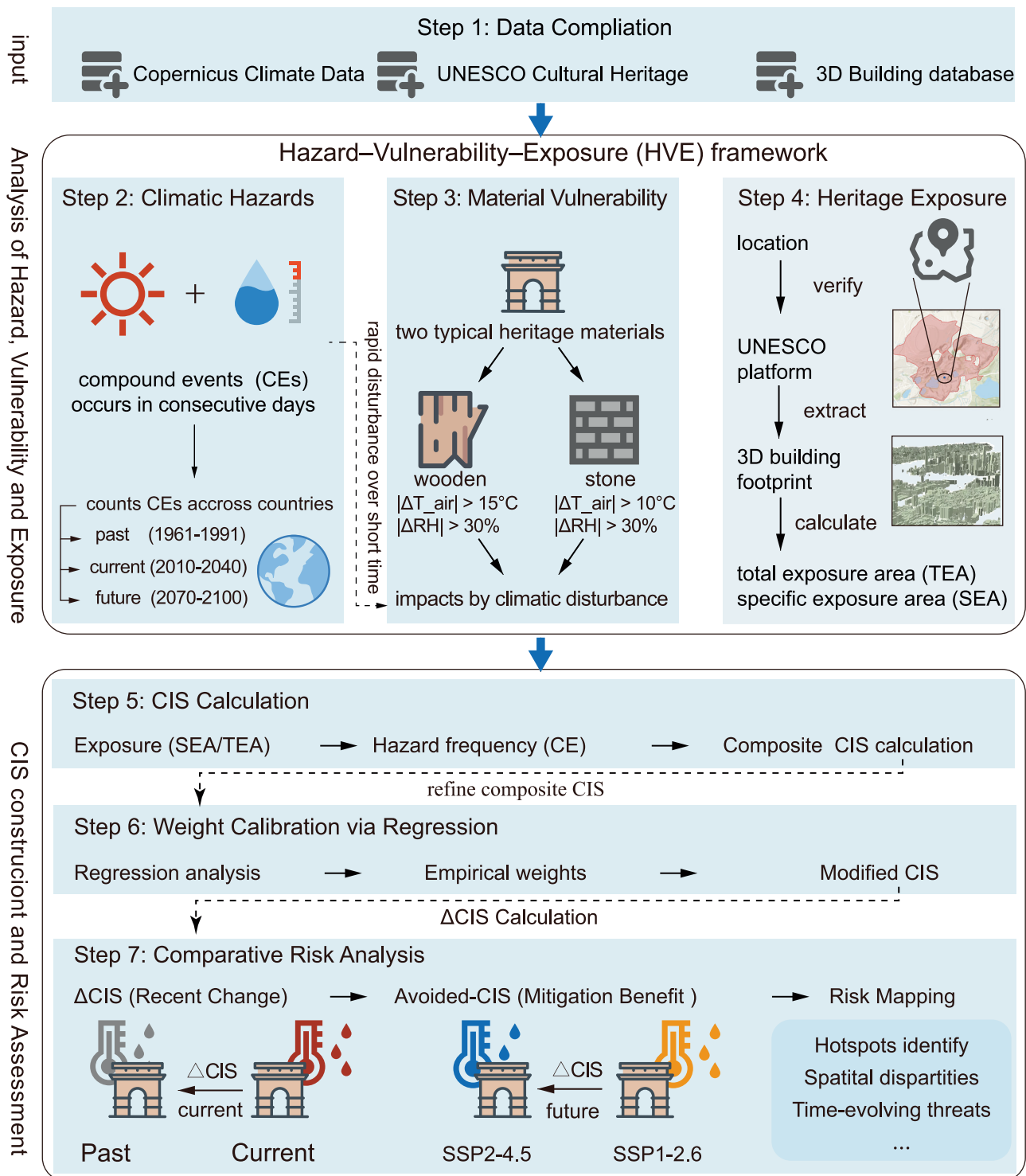


Fig. 6 | The hazard–vulnerability–exposure (HVE) framework and CIS assessment process. The flowchart summarizes seven consecutive steps: (1) data compilation; (2–4) evaluation of compound climatic hazards, material-specific vulnerability (stone, wood) and site exposure (total and specific exposed area, TEA

and SEA); (5–6) calculation of composite CIS and empirical weight calibration; (7) comparative risk analysis for historical, current and future low- (SSP1–2.6) and medium-emission (SSP2-4.5) scenarios.

climate-induced events.

$$CIS_{iTEA} = TEA_i * CE_i \quad (5)$$

$$CIS_{iSEA} = SEA_i * CE_i \quad (6)$$

To determine how strongly exposure and hazard contribute, we fitted a fixed-effects panel regression:

$$CIS_{it} = \beta_o + \beta_{SEA}SEA_i + \beta_{CE}CE_{i,t} + \beta_{SEA*CE}(SEA_iCE_{i,t}) + \gamma_{current}\delta_{current} + \gamma_{future}\delta_{future} + \theta_{current}(\delta_{current}CE_{i,t}) + \theta_{future}(\delta_{future}CE_{i,t}) + \mu_i + \epsilon_{i,t} \quad (7)$$

Table 2 | Material-specific temperature and humidity thresholds used to count CEs

Material	Typical fabric	$ \Delta T $ Threshold	$ \Delta RH $ Threshold	Damage	Key References
Stone	sandstone, masonry, marbles	$\sim 10^\circ\text{C}$ rapid cycles	30–70% rapid cycles	freeze-thaw cycles, surficial damage, thermal micro-cracking, black-crust, indoor thermal stress	13,23,50,51,56,57
Wood	embedded beam heads	$\sim 15^\circ\text{C}$ rapid cycles	30–70% rapid cycles	decay mechanical damage biodegradation	13,23,55

where t indexes the three 30-year slices, δ are time-period dummies, and μ are site fixed effects. β_{SEA} and β_{CE} capture the main effects of exposure and hazard. γ and θ measure level and slope shift relative to the baseline period (1961–1990). Coefficients remain significant and retain their signs after winsorising the top and bottom 1% of SEA and CE values, indicating that results are not driven by outliers. The estimated coefficients are then used as weights to produce the final, site-specific CIS values employed in Step 6.

Step 6. Weight calibration via regression

To refine the preliminary CIS values, we estimated a fixed-effects panel regression that relates exposure (SEA), hazard frequency (CE), and their interaction to the initial CIS values (Eq. 8). The fitted coefficients provide empirical weights for each component.

$$\text{CIS}_{i,\text{modified}} = \beta_0 + \beta_{\text{SEA}} \text{SEA}_i + \beta_{\text{CE}} \text{CE}_{i,t} + \beta_{\text{SEA} \times \text{CE}} (\text{SEA}_i \text{CE}_{i,t}) + \gamma_t + \theta_t (\delta_t \text{CE}_{i,t}) \quad (8)$$

$\text{CIS}_{i,\text{modified}}$ values are computed for each heritage site across each period and emission scenario and serve as the basis for final index generation in Step 7.

Step 7. Comparative risk analysis

We evaluated how climate risk evolves by comparing CIS values across periods and emission pathways^{12,23,37}.

- **Recent change:** We subtracted the baseline mean (1961–1990) from the present-day mean (2010–2040) for each site to obtain $\Delta \text{CIS}_{\text{current-past}}$ (Eq. 9).
- **Future mitigation benefit:** We subtracted the low-emission projection (SSP1-2.6, 2070–2100) from the medium-emission projection (SSP2-4.5, 2070–2100) to obtain $\Delta \text{CIS}_{\text{SSP245-SSP126}}$ (Eq. 10).

$$\Delta \text{CIS}_{\text{current-past}} = \text{CIS}_{i,\text{modified_current}} - \text{CIS}_{i,\text{modified_past}} \quad (9)$$

$$\Delta \text{CIS}_{\text{SSP245-SSP126}} = \text{CIS}_{i,\text{modified_SSP245}} - \text{CIS}_{i,\text{modified_SSP126}} \quad (10)$$

To visualize the results, ΔCIS outcome is classified with natural breaks (Jenks) into four site-specific classes: rare impact (<0), stable ($0 \leq Q_2$), moderate ($Q_2 < Q_3$), Severe (for threats)/Major (for positive avoided-CIS) ($\geq Q_3$). Mapping the classified ΔCIS values highlight hotspots where climate pressure on heritage is intensifying or where substantial Avoided-CIS benefits could occur (Figs. 2 and 3), and further reveal national disparities in threats and mitigation benefit (Figs. 4 and 5). For completeness we also calculated $\Delta \text{CIS}_{\text{SSP245-current}}$ —the change from today's climate window (2010–2040) to the medium emission future (SSP2-4.5)—and present the resulting map in Supplementary Fig. 2.

Future scenario simulation

Shared socioeconomic pathways (SSPs) is a set of pathways for modeling future societal developments that are closely related to the impacts of climate change and the formulation of climate policy. In this study, we mainly focus on SSP1-2.6 and SSP2-4.5—two scenarios widely used in IPCC WG-II to frame risk assessments. SSP1-2.6 represents a Paris-aligned low-emission future ($<2^\circ\text{C}$), capturing the most ambitious yet still technically plausible pathway; SSP2-4.5 reflects current global policy commitments ($\approx 2.7^\circ\text{C}$) and therefore the trajectory most relevant for low- and middle-income regions.

High-emission pathways such as SSP3-7.0 and SSP5-8.5 are not included in our main analysis because they represent extreme pathway with limited relevance to the current policy dilemmas of heritage governance—namely, the challenge of balancing realistic mitigation efforts (SSP2-4.5) against long-term aspirational goals (SSP1–2.6). Nonetheless, our framework is fully compatible with open-access climate datasets under all SSPs, and can be readily extended by other researchers seeking to evaluate heritage risks under more severe emission futures.

AI declaration

This study made limited, transparent use of ChatGPT for two strictly supporting purposes. First, ChatGPT suggested improvements to sentences, focusing on grammar, clarity, tone, and concision. Second, ChatGPT provided Python snippets that automate daily extraction of temperature and humidity series for each UNESCO site from large global climate datasets. The authors integrated, tested, and debugged Python snippets within their own analysis pipeline. All scientific ideas, arguments, and interpretations were conceived and drafted by the authors.

Data availability

All data that support the findings of this study are publicly accessible. Global 3-D building footprints are available on Zenodo (<https://doi.org/10.5194/essd-16-5357-2024>)³⁵. Historical and contemporary climate fields come from the Copernicus Climate Data Store: ERA5-Land (<https://doi.org/10.24381/cds.e2161bac>)⁴⁷ and CMIP6 projections (<https://doi.org/10.24381/cds.c866074c>)⁴⁸. UNESCO World Heritage List were downloaded from the official World Heritage List (<https://whc.unesco.org/en/list>). Derived products generated in this study are archived on Figshare: site-level daily temperature and humidity values (<https://doi.org/10.6084/m9.figshare.28938377>)⁵⁹ and site-clipped 3-D building shapefiles (<https://doi.org/10.6084/m9.figshare.28912334>)⁶⁰.

Code availability

The Python script used to extract the daily climate series is openly available on Figshare, together with the extracted climate data, under <https://doi.org/10.6084/m9.figshare.28938377>⁵⁹. There are no restrictions on the use of these data or code.

Received: 19 February 2025; Accepted: 18 July 2025;

Published online: 05 August 2025

References

1. Chen, G. et al. Natural world heritage sites are at risk from climate change globally. *Commun. Earth Environ.* **5**, 760 (2024).
2. Colette, A. *Climate Change and World Heritage: Report on Predicting and Managing the Impacts of Climate Change on World Heritage And Strategy to Assist States Parties to Implement Appropriate Management Responses*. <https://unesdoc.unesco.org/ark:/48223/pf0000160019> (2007).
3. Sesana, E., Gagnon, A. S., Ciantelli, C., Cassar, J. & Hughes, J. J. Climate change impacts on cultural heritage: a literature review. *Wiley Interdisciplinary Reviews-Climate Change*. **12**, <https://doi.org/10.1002/wcc.710> (2021).
4. Climate Change and Heritage Working Group. The future of our pasts: engaging cultural heritage in climate action outline of climate change

- and cultural heritage. https://www.opr.ie/wp-content/uploads/2021/03/ICOMOS173TheFutureofourPastsFinal-compressed_compressed.pdf (2019).
5. UNESCO. *Policy Document on Climate Action for World Heritage*. <https://whc.unesco.org/en/documents/204421> (2023).
6. Perry, J. & Falzon, C. *Climate Change Adaptation for Natural World Heritage Sites: A Practical Guide*. <https://unesdoc.unesco.org/ark:/48223/pf0000227613> (2014).
7. Orr, S. A., Richards, J. & Fatoric, S. Climate change and cultural heritage: a systematic literature review (2016–2020). *Hist. Env. -Policy Pract.* **12**, 434–477 (2021).
8. Simpson, N. P. et al. Decolonizing climate change–heritage research. *Nat. Clim. Chang.* **12**, 210–213 (2022).
9. Fatorić, S. & Seekamp, E. Are cultural heritage and resources threatened by climate change? A systematic literature review. *Clim. Chang.* **142**, 227–254 (2017).
10. Voudoukas, M. I. et al. African heritage sites threatened as sea-level rise accelerates. *Nat. Clim. Change* **12**, 256–262 (2022).
11. Hu, H. Impact of climatic-meteorological conditions on Polish wooden cultural heritage: an example of world heritage sites featuring wooden churches near Krakow. *Human. Soc. Sci. Commun.* **11**, 1318 (2024).
12. Lin, B. B. B. et al. Holistic climate change adaptation for World Heritage. *Nat. Sustain.* **6**, 1157–1165 (2023).
13. Blavier, C. L. S. et al. Adaptive measures for preserving heritage buildings in the face of climate change: a review. *Build. Environ.* **245**, 110832 (2023).
14. Chen, Z. H., Gao, Q., Li, X. W., Yang, X. H. & Wang, Z. B. Beyond inundation: a comprehensive assessment of sea level rise impact on coastal cultural heritage in China. *Herit. Sci.* **12**, 121 (2024).
15. Reimann, L., Vafeidis, A. T., Brown, S., Hinkel, J. & Tol, R. S. Mediterranean UNESCO World Heritage at risk from coastal flooding and erosion due to sea-level rise. *Nat. Commun.* **9**, 4161 (2018).
16. Li, Y. et al. The potential impact of rising sea levels on China's coastal cultural heritage: a GIS risk assessment. *Antiquity* **96**, 406–421 (2022).
17. Lollino, G. & Audisio, C. UNESCO World Heritage sites in Italy affected by geological problems, specifically landslide and flood hazard. *Landslides* **3**, 311–321 (2006).
18. Margottini, C. & Vilímek, V. The ICL Network on “Landslides and Cultural & Natural Heritage (LACUNHEN)”. *Landslides* **11**, 933–938 (2014).
19. Falk, M. T. & Hagsten, E. Assessing different measures of fire risk for Cultural World Heritage Sites. *Herit. Sci.* **11**, <https://doi.org/10.1186/s40494-023-01026-y> (2023).
20. Hollesen, J., Jepsen, M. S., Stendel, M. & Harmsen, H. Assessing the consequences of recent climate change on World Heritage sites in South Greenland. *Sci. Rep.* **14**, 9732 (2024).
21. Hu, H. & Hewitt, R. J. Understanding climate risks to world cultural heritage: a systematic analysis and assessment framework for the case of Spain. *Herit. Sci.* **12**, 194 (2024).
22. Leissner, J. et al. Climate for Culture: assessing the impact of climate change on the future indoor climate in historic buildings using simulations. *Herit. Sci.* **3**, 38 (2015).
23. Frasca, F. et al. Assessing microclimate thresholds for heritage preventive conservation to achieve sustainable and energy efficiency goals in a changing climate. *Sci. Rep.* **14**, 18707 (2024).
24. Ireland, T., Brown, S. & Schofield, J. Situating (in)significance. *Int. J. Herit. Stud.* **26**, 826–844 (2020).
25. Petzold, J., Andrews, N., Ford, J. D., Hedemann, C. & Postigo, J. C. Indigenous knowledge on climate change adaptation: a global evidence map of academic literature. *Environ. Res. Lett.* **15**, <https://doi.org/10.1088/1748-9326/abb330> (2020).
26. DeSilvey, C. & Harrison, R. Anticipating loss: rethinking endangerment in heritage futures. *Int. J. Herit. Stud.* **26**, 1–7 (2020).
27. Sesana, E., Gagnon, A. S., Bonazza, A. & Hughes, J. J. An integrated approach for assessing the vulnerability of World Heritage Sites to climate change impacts. *J. Cult. Herit.* **41**, 211–224 (2020).
28. Lafrenz Samuels, K. & Platts, E. J. Global climate change and UNESCO World Heritage. *Int. J. Cult. Prop.* **29**, 409–432 (2022).
29. Terrill, G. Climate change: how should the World Heritage Convention respond? *Int. J. Herit. Stud.* **14**, 388–404 (2008).
30. Fatorić, S. & Biesbroek, R. Adapting cultural heritage to climate change impacts in the Netherlands: barriers, interdependencies, and strategies for overcoming them. *Clim. Chang.* **162**, 301–320 (2020).
31. Cacciotti, R. et al. Climate change-induced disasters and cultural heritage: optimizing management strategies in Central Europe. *Clim. Risk Manag.* **32**, 100301 (2021).
32. Seekamp, E. & Jo, E. Resilience and transformation of heritage sites to accommodate for loss and learning in a changing climate. *Clim. Chang.* **162**, 41–55 (2020).
33. Korai, H., Kojima, Y. & Suzuki, S. Bending strength and internal bond strength of wood-based boards subjected to various exposure conditions. *J. Wood Sci.* **61**, 500–509 (2015).
34. Corvo, F. et al. Influence of air pollution and humidity on limestone materials degradation in historical buildings located in cities under tropical coastal climates. *Water, Air, Soil Pollut.* **205**, 359–375 (2010).
35. Che, Y. et al. 3D-GloBFP: the first global three-dimensional building footprint dataset. *Earth Syst. Sci. Data* <https://doi.org/10.5194/essd-16-5357-2024> (2024).
36. Gao, J. & O'Neill, B. C. Mapping global urban land for the 21st century with data-driven simulations and Shared Socioeconomic Pathways. *Nat. Commun.* **11**, 2302 (2020).
37. Ridder, N. N., Ukkola, A. M., Pitman, A. J. & Perkins-Kirkpatrick, S. E. Increased occurrence of high impact compound events under climate change. *npj Clim. Atmos. Sci.* **5**, 3 (2022).
38. Bonazza, A. et al. Safeguarding cultural heritage from climate change related hydrometeorological hazards in Central Europe. *Int. J. Disaster Risk Reduct.* **63**, 102455 (2021).
39. Ridder, N. N. et al. Global hotspots for the occurrence of compound events. *Nat. Commun.* **11**, 5956 (2020).
40. Sobie, S. R., Zwiers, F. W. & Curry, C. L. Climate model projections for Canada: a comparison of CMIP5 and CMIP6. *Atmos. Ocean* **59**, 269–284 (2021).
41. Sillmann, J., Kharin, V. V., Zwiers, F. W., Zhang, X. & Bronaugh, D. Climate extremes indices in the CMIP5 multimodel ensemble: part 2. Future climate projections. *J. Geophys. Res. Atmos.* **118**, 2473–2493 (2013).
42. Almazroui, M. et al. Projected changes in climate extremes using CMIP6 simulations over SREX regions. *Earth Syst. Environ.* **5**, 481–497 (2021).
43. Vogel, M. M., Hauser, M. & Seneviratne, S. I. Projected changes in hot, dry and wet extreme events' clusters in CMIP6 multi-model ensemble. *Environ. Res. Lett.* **15**, 094021 (2020).
44. Marszałek, M., Dudek, K. & Gawel, A. Black crust from historic buildings as a natural indicator of air pollution: a case study of the Lipowiec Castle, Babice, Southern Poland. *Sustainability* **16**, 3816 (2024).
45. Labadi, S., Giliberto, F., Rosetti, I., Shetabi, L. & Yildirim, E. Heritage and the sustainable development goals: policy guidance for heritage and development actors. *Paris: International Council on Monuments and Sites (ICOMOS)* (2021).
46. Paolini, A. et al. Risk management at heritage sites: a case study of the petra world heritage site. <https://unesdoc.unesco.org/ark:/48223/pf0000217107> (2012).
47. Muñoz Sabater, J. ERA5–Land hourly data from 1950 to present. Copernicus Climate Change Service (C3S) data Climate Data Store (CDS) <https://doi.org/10.24381/cds.e2161bac> (2019).

48. Copernicus Climate Change Service, C. D. S. CMIP6 climate projections: Copernicus Climate Change Service (C3S) Climate Data Store (CDS). <https://doi.org/10.24381/cds.c866074c> (2021).
49. Shi, Q. et al. The last puzzle of global building footprints—mapping 280 million buildings in East Asia based on VHR images. *J. Remote Sens.* **4**, 0138 (2024).
50. Chen, G., Wan, Y., Li, Y., Pei, X. & Huang, D. Time-dependent damage mechanism of rock deterioration under freeze–thaw cycles linked to alpine hazards. *Nat. Hazards* **108**, 635–660 (2021).
51. Metals, M., Palcikovskis, A., Borodinecs, A. & Lesinskis, A. Typology of Latvian churches and preliminary study on indoor air temperature and moisture behavior. *Buildings* **12**, 1396 (2022).
52. Rajcic, V., Skender, A. & Damjanovic, D. An innovative methodology of assessing the climate change impact on cultural heritage. *Int. J. Archit. Herit.* **12**, 21–35 (2018).
53. Mayr, S., Gruber, A. & Bauer, H. Repeated freeze–thaw cycles induce embolism in drought stressed conifers (Norway spruce, stone pine). *Planta* **217**, 436–441 (2003).
54. Ashley-Smith, J. Climate for Culture: D 4.2. *Report on Damage Functions in Relation to Climate Change and Microclimatic Response*, accessed 11 September 2018. Available online: <https://www.climateforculture.eu/>.
55. Vandemeulebroucke, I., Kotova, L., Caluwaerts, S. & Van Den Bossche, N. Impact of climate change on degradation risks in solid masonry walls: uncertainty assessment using a multi-model ensemble. *Build. Environ.* **264**, 111910 (2024).
56. Sorrentino, B., Screpanti, A. & De Marco, A. Corrosion on cultural heritage buildings in Jordan in current situation and in future climate scenarios. *Sci. Rep.* **14**, 25373 (2024).
57. Waragai, T. Influence of thermal cycling in the mild temperature range on the physical properties of cultural stones. *J. Cult. Herit.* **59**, 171–180 (2023).
58. Akkurt, G. G. et al. Dynamic thermal and hygrometric simulation of historical buildings: critical factors and possible solutions. *Renew. Sustain. Energy Rev.* **118**, 109509 (2020).
59. Wu, Y. J. Climate dataset for UNESCO World Heritage Sites. figshare. Dataset. <https://doi.org/10.6084/m9.figshare.28938377.v3> (2025).
60. Wu, Y. J. UNESCO Cultural Heritage 3D Building Dataset. figshare. Dataset. <https://doi.org/10.6084/m9.figshare.28912334.v1> (2025).

Acknowledgements

This work was supported by the National Social Science Fund of China, General Program (Grant 24BMZ054, H.C.).

Author contributions

Zihua Chen conceived the idea and led the research framework design. Qian Gao and Yajing Wu designed the study. Zihua Chen, Yajing Wu, Jiaxin Li, and Xiaowei Li performed data collection. Zihua Chen, Qian Gao, Yajing Wu, Zhenbo Wang and Xiao Li conducted data analysis and interpretation. Haiyang Cui supervised methodology refinement and provided funding support. Zihua Chen, Qian Gao, and Yajing Wu drafted the manuscript; all authors reviewed and approved the final version.

Competing interests

The authors declare no competing interests.

Ethics approval

This study was conceived, designed and carried out entirely by the authors, all of whom are affiliated with Chinese research institutions. The work relied exclusively on publicly available global datasets (Copernicus ERA5 climate reanalysis, the UNESCO World Cultural Heritage List, and open building-footprint data) and involved no fieldwork, human participants, animals or export of biological or cultural material; therefore local ethics-review approval and benefit-sharing agreements were not required. All contributors who satisfied the authorship criteria are listed as authors, and their roles were agreed upon before analysis began; no additional contributors need acknowledgement. The research questions and interpretations were discussed with colleagues at the data-providing institutes to ensure local and global relevance. To support capacity-building in other regions, all code and derived datasets are publicly deposited on Figshare.

Additional information

Supplementary information The online version contains supplementary material available at <https://doi.org/10.1038/s43247-025-02603-8>.

Correspondence and requests for materials should be addressed to Haiyang Cui.

Peer review information *Communications Earth & Environment* thanks DPP Meddage, Xiaoyang Zhong and Daniel Hoomweg reviewer(s) for their contribution to the peer review of this work. Primary Handling Editors: Mengze Li and Martina Grecequet. A peer review file is available.

Reprints and permissions information is available at <http://www.nature.com/reprints>

Publisher's note Springer Nature remains neutral with regard to jurisdictional claims in published maps and institutional affiliations.

Open Access This article is licensed under a Creative Commons Attribution-NonCommercial-NoDerivatives 4.0 International License, which permits any non-commercial use, sharing, distribution and reproduction in any medium or format, as long as you give appropriate credit to the original author(s) and the source, provide a link to the Creative Commons licence, and indicate if you modified the licensed material. You do not have permission under this licence to share adapted material derived from this article or parts of it. The images or other third party material in this article are included in the article's Creative Commons licence, unless indicated otherwise in a credit line to the material. If material is not included in the article's Creative Commons licence and your intended use is not permitted by statutory regulation or exceeds the permitted use, you will need to obtain permission directly from the copyright holder. To view a copy of this licence, visit <http://creativecommons.org/licenses/by-nc-nd/4.0/>.

© The Author(s) 2025